Original Scientific Article Journal of Decision Analytics and Intelligent Computing
Vol. 5 issue 1, (2025) 259-274 https://doi.org/10.31181/jdaic10026122025d

DriDrowsy: An enhanced framework for drowsiness detection

Soma Datta[1,*] and Moumita Shee[1]

[1] Department of Computer Science and Engineering, Sister Nivedita University, Kolkata, India

* Correspondence: soma.da@snuniv.ac.in

Received 27 May 2025
Accepted for publication 16 December 2025
Published 26 December 2025

Abstract

Road accidents remain one of the leading causes of non-natural deaths worldwide, and driver distraction is a major contributor. Among the various forms of distraction, drowsiness is particularly dangerous as it greatly increases the likelihood of traffic collisions. Detecting drowsiness early and issuing timely alerts can help prevent such incidents by encouraging drivers to take necessary breaks. This paper presents an image-based drowsiness detection method that utilizes the Eye Aspect Ratio (EAR) and Mouth Opening Ratio (MOR) in combination with a modified Haar Cascade model. The system detects facial indicators of drowsiness that include yawning, closed eyelids, and partially closed eyes through thresholding and expression analysis. Experimental results show that the method achieves an accuracy of over 96.75% in identifying drowsy states. This proposed method is experimentally tested on three different benchmarked data sets. By consistently monitoring driver alertness, this approach offers a promising solution for reducing fatigue-related road accidents and enhancing overall driving safety.

Keywords: Eye Aspect Ratio (EAR), facial features, image pre-processing, haar cascade, object detection, image segmentation, Mouth Opening Ratio (MOR).

1. Introduction

According Lenin et al. (2021) and ANSI/ASHRAE Standard 55 (2023) to the World Health Organization (WHO), road accidents cause approximately 1.35 million deaths and 20-50 million serious injuries each year, ranking among the top ten global causes of mortality and serving as the leading cause of death for individuals aged 5-29 (Global status report on road safety 2018, 2018; Chen et al., 2021). These incidents also impose substantial economic losses, estimated at nearly USD 1.8 trillion between 2015 and 2030 (Chen et al., 2021), and projections indicate that this burden will continue to rise (Global status report on road safety 2018, 2018). Driver drowsiness is a major contributor to these accidents, especially among individuals who drive for extended periods, such as truck and bus operators. Fatigue resulting from insufficient sleep or prolonged driving significantly reduces alertness and increases crash risk. Globally, drowsy driving is linked to an estimated 70000 to 80000 injuries and 1000 to 2000 confirmed fatalities annually, with actual numbers likely underreported. Therefore, effective detection of driver drowsiness and timely alert mechanisms are critical for mitigating fatigue- related accidents and enhancing road safety. Certain natural behaviors, like eye closure, yawning, blinking, and head posture, can

be used to detect tiredness (Rastogi and Ryuh, 2019). To capture photo of driver from different angle required installation of camera in front of the devices (Horne and Reyner, 1999). After that, more processing is done on the driver's photos to determine how sleepy they are. This can be accomplished by using image processing to do real-time Eye Aspect Ratio (EAR) monitoring.

The Figure 1 shows a driver-monitoring workflow in which a car-mounted camera captures video frames, detects and segments the driver's face, and extracts key facial features for analysis. After processing these features to assess the driver's state, the system generates real-time alerts when needed and discards the processed frames. The major contributions of this research work are summarized as follows:

a) First, it introduces a modified approach for computing the Eye Aspect Ratio (EAR) and Mouth Opening Ratio (MOR) to detect drowsiness by identifying eye landmarks through a hybrid method that combining 68-facial-landmark model and the Haar Cascade model.
b) Second, it presents a yawn-detection mechanism that evaluates the Euclidean distance between upper and lower lip landmarks using Dlib's pre-trained facial-landmark model.
c) The authors achieved average EAR values of 0.339 for open eyes and 0.141 for closed eyes, and the system successfully triggered real-time alerts whenever the EAR dropped below the defined threshold, providing immediate notification to the driver.

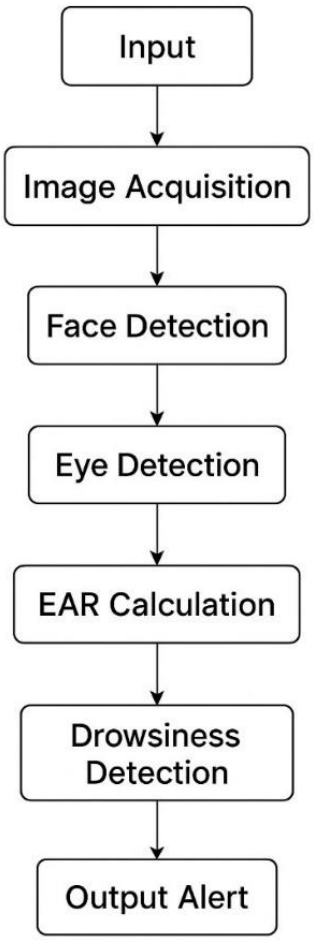

Figure 1. Functional Diagram

These contributions highlight our efforts to address the safety, maintenance, and accessibility challenges faced by vehicle owners in India, offering a scalable, cost-effective, and user-centric solution. This paper contains mainly four sections. Introduction is described in section 1. Section 2 contains the literature survey along with its limitations. The design of the proposed technique is described in section 3. Result is described in detail in section 4 followed by conclusions.

2. Literature Survey of the Existing methods on Same Domains

Drowsiness and its effects on drivers have been the subject of extensive research over the past 20 years, which has revealed important consequences like decreased mental alertness and awareness, a diminished capacity to operate a vehicle safely, an increased risk of human error that could result in injuries or fatalities, slower reaction times, and impaired judgment (Horne and Reyner, 1999; Dua et al., 2018; Rastogi and Ryuh, 2019). According to studies, getting enough sleep before driving and taking frequent breaks ideally quick naps during lengthy journeys often accompanied by caffeine consumption like a cup of coffee are the most successful preventative measures (Moujahid et al., 2021; Magán et al., 2022). Drivers who fall asleep are unlikely to remember doing so until it is too late, according to Horne and Reyner (1999). They simply remember the sense of growing tiredness that precedes an accident (i.e., resisting sleep). As a result, transportation researchers are becoming more interested in creating intelligent systems that can identify driver fatigue early on. In Horne and Reyner (1999), a machine learning based drowsiness detection technique has been proposed. The accuracy of this method is 87%. In this paper, a novel real time-based driver drowsiness detection is being proposed to identify the eye movement and face recognition. The system compares extracted eye images with a dataset to determine drowsiness. An alarm sounds if the eyes have been closed for a specified period of time in order to warn the driver. The system continuously tracks eye status, adjusting a score based on whether the eyes are open or closed. This paper aims to achieve 80% accuracy in drowsiness detection to help reduce road accidents. Two Node Splits and Random Forest Regression are utilized to identify Euclidean and face traits. Eye closure and yawning are measured to assess the sleepiness condition using distance measures for the lips and eyes (Rastogi and Ryuh, 2019). In Bakheet and Al-Hamadi (2021), the authors have described a face monitoring system using a compact face texture descriptor. It is able to cover the most discriminant drowsy features. The compactness has been achieved by both a multi-scale pyramidal face representation that capture the main characteristics of local and global information, and the feature selection process applied on the raw extracted features. In order to prevent traffic accidents, Zhang et al. (2012) introduce an Advanced Driving Assistance System (ADAS) that detects driver drowsiness in a non-intrusive manner. Two approaches are designed to reduce false positives using 60-second face-visible image sequences: one integrates deep learning feature extraction with a fuzzy logic-based judgment system, and the other combines recurrent and convolutional neural networks. Kolus et al. (2023) examines the empirical research and published literature on driver drowsiness detection systems that rely on eye activity (DDD systems). Preferred reporting items for systematic reviews and meta-analyses served as the foundation for this study's methodology. The review looked into the various assessment techniques that gauged the eye activity of a subject to drowsiness and it developed a registry discerning mapping of the techniques. It also processed eye measuring technologies available today. Decision making systems designed to classify and foresee the level of drowsiness. Finally, the study provided a little perspective for the advance of eye activity measures on drowsiness detection systems learning from actual behaviours creating the basis for further development of this system (Choudhury et al., 2023). These studies highlight the reliability of drowsiness detection systems. The limitations are listed in Table 1. These studies highlight the reliability of drowsiness detection systems.

Table 1. Limitations associated with specific existing methods

Sl number	Used Techniques	Accuracy	Limitation
1	Monitors drowsiness using video feed (Dua et al., 2018).	The system achieved an overall facial feature detection accuracy of 85%.	Tested on a limited number of subjects (20), which may affect the generalizability.
2	Drivers' Face Tracking: Utilizes the Viola-Jones method (Singh et al., 2023).	Rate of approximately 93% during testing	The Viola-Jones method fails when frontal facial region of the driver is not positioned directly in front of the camera
3	Day and Night Systems: Operates using digital cameras and near- infrared (NIR) illumination for day and night (Mohana and Sheela Rani, 2019)	Achieved over 90% accuracy for both open and closed states	Variations in illumination can result in partial information and the effectiveness of eye detection can be compromised under rapidly changing lighting conditions.
4	Conversion of images to black and white, background elimination techniques using HSV conversion, morphological processing (Kolus, 2024).	Accuracy level is moderate.	Current processing methods may suffer from limitations in handling images under poor visibility
5	In Ed-Doughmi et al. (2020), the authors proposed a technique based on video oculography to identify eye blinking.	92%	Not able to detect eye blinking if hair covers some little portion of eye.
6	Zhang et. al. (2012) proposed a technique based on mixed effect ordered logit model.	62.84%	Not well for the real time scenario as it's accuracy is less.
7	In Bakheet and Al-Hamadi (2021), authors reported a technique based on histogram orientation and gradient features.	85.62%	Not well for the real time scenario

3. Proposed Method

In order to track driver behavior in real time, authors have attempted to concentrate on a process that must be able to precisely assess continuous data, such as eye movements, facial expressions, and driving patterns. False positives or negatives in the detection of drowsiness could lead to missed warning signs or unnecessary cautions, both of which are undesirable. Figure 2 illustrates a complete workflow for a video-based drowsiness-detection system. It begins with either recorded or real-time video, from which frames are extracted and converted into two-dimensional images. Face region detection is applied to each image, followed by marking facial landmarks within the segmented regions. From these landmarks, the system identifies the eye and mouth regions to compute

the Eye Aspect Ratio (EAR) and Mouth Opening Ratio (MOR). Using the first 250 frames, an initial threshold value is established. The system then monitors for yawning and head bending; if either is detected, the threshold value is adjusted accordingly. Finally, the EAR is compared against the current threshold to determine whether the user is drowsy, leading to either "drowsiness detected" or "drowsiness not detected".

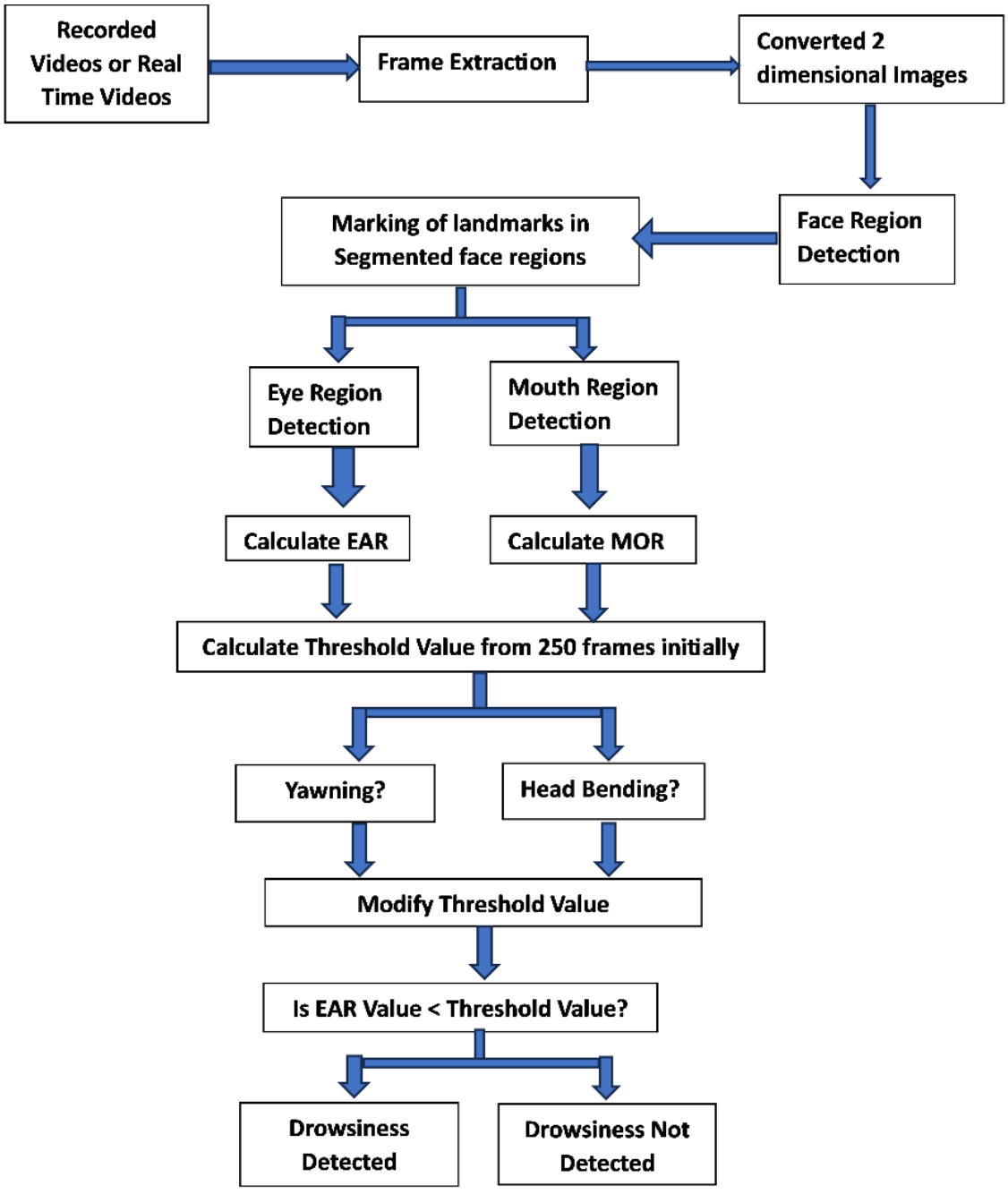

Figure 2. Functional Diagram

3.1 Dataset Details

This subsection describes the list of datasets in table form. All these datasets are used in this research work for experimental purpose, Table 2.

Table 2. Dataset Details

SL number	Database Name	Total Data	Class Distribution	Features
1	Drowsiness Detection Dataset (Patil, 2020; Jebraeily, 2023)	4000	Closed Eyes: 2000 images, Open Eyes: 2000 images.	Eye Aspect Ratio (EAR), Eye Closure Degree, Facial Landmark-Based Features (distances and angles between landmarks)
2	Hazem Fahmy Dataset (Fahmy, 2023)	4232	Closed Eyes: 2190 images, Opened Eyes: 2042 images	Eye Aspect Ratio (EAR), Eye closure Degree, Facial Landmark- Based Features
3	Detection for Drowsiness Detection (Fahmy, 2023)	5220	Yawn and non-yawn	Mouth Aspect Ratio (MAR), Mouth Width, Mouth Height, Mouth Area, Facial Landmark- Based Features, Distances between key landmarks (example - tip of nose, eyes etc.)

3.2 Data Acquisition

A laptop webcam is used to first record the video, and then the laptop extracts and processes the frames. After the frames are acquired, the required driver-related data is extracted by applying image-processing algorithms to the two-dimensional images created from the recorded video. Volunteers are told to look at the camera and do things like yawning their mouths, bending their heads, and repeatedly blinking and closing their eyes. The webcam is set up so that it can capture these activities for 10 to 15 minutes. This process has been continued for first time experimental purpose. After getting good accuracy, the 3 different datasets described in table 2 have been also verified.

3.3 Face Region Detection

Figure 3 illustrates the workflow for face-region detection using Haar cascade classifiers with basic preprocessing.

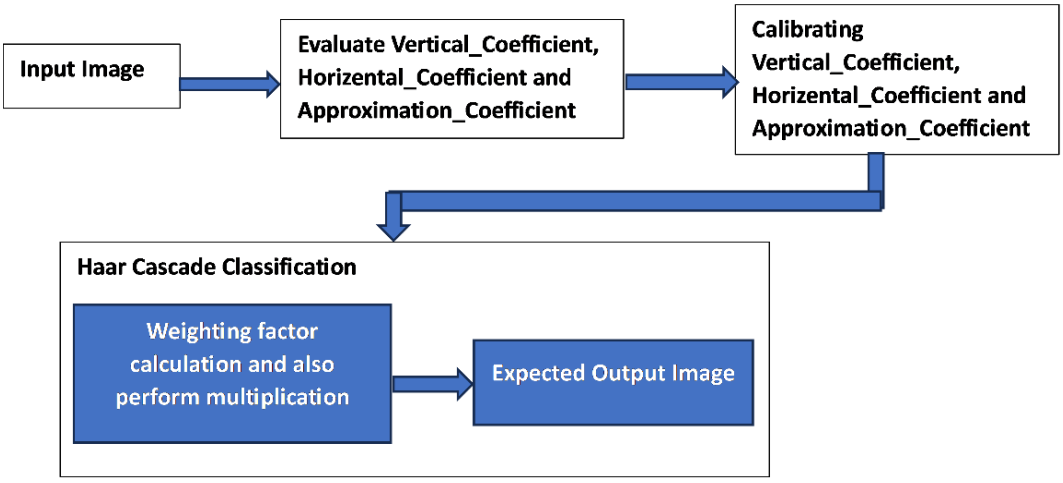

Figure 3. Flow Diagram of Face Region Detection

As the first step in drowsiness detection, the method calibrates an image's vertical and horizontal components to preserve essential edge information for frontal face identification. The calibrated image is then passed through the Haar cascade classifier, where sub-window operations compute feature values; a face is detected when these values satisfy all classifier stages. If a sub-window fails, processing moves to the next pixel. By enhancing vertical components, the method ensures that key edge details are retained for more accurate detection. The mathematical expressions for the approximation and detail coefficients follow.

$$I_{aprox}(x,y)=\sum_{i_1=0}^{K-1}\sum_{i_2=0}^{K-1} g(i_1)*g(i_2)*I(2x-i_1,2y-i_2) \tag{1}$$

$$I_{hori}(x,y)=\sum_{i_1=0}^{K-1}\sum_{i_2=0}^{K-1} g(i_1)*h(i_2)*I(2x-i_1,2y-i_2) \tag{2}$$

$$I_{vert}(x,y)=\sum_{i_1=0}^{K-1}\sum_{i_2=0}^{K-1} h(i_1)*g(i_2)*I(2x-i_1,2y-i_2) \tag{3}$$

Here, $g(i_1)$ and $g(i_2)$ are scaling functions. The filter length of the transformation functions is represented by K. $h(i_1)$ and $h(i_2)$ are the wavelet function. $I(2x\text{-}i_1, 2y\text{-}i_2)$ is the input image. $I_{aprox}(x, y)$, $I_{vert}(x, y)$, $I_{hori}(x, y)$ are representing approximated detailed coefficient, vertical detailed coefficient and horizontal detailed co- efficient respectively. The wavelet function in the column direction and the scaling function in the row direction are used to get the horizontal detail coefficient. The scaling function in the column direction and the wavelet function in the row direction are used to get the vertical detail coefficient (Datta et al., 2015; Choudhury et al., 2023; Biswas et al., 2023). The threshold value is used to calibrate the vertical detail coefficient to zero through a one-level transformation procedure, while the zero-calibrated vertical detail coefficient is used as the threshold value to calibrate the horizontal detail coefficient to zero. Prior to calibrating from the approximation detail coefficient, the vertical and horizontal detail coefficients must be set to zero in order to provide the appropriate image for Haar cascade classifiers. Equation (4) is a mathematical expression for the zero calibrated vertical, horizontal detail coefficient, and desired image. Here $\text{Img}_{vert}(x, y)$ is the zero-calibrated vertical detail coefficient, $\text{Img}_{HR}(x, y)$ is the zero-calibrated horizontal detail coefficient, $\text{Img}_{desire}(x, y)$ is the desired image, that preserves the appropriate edge in- formation of the face detection using the Haar cascade classifiers. α is weighting factor. When a grayscale image gets darker, the pixel value gets closer to zero, and when it gets brighter, it gets closer to 255. Because the computing procedure includes subtracting the adjacent pixels at each coordinate, the vertical and horizontal detail coefficients can have both positive and negative values. The accumulated value in the bright and dark areas of the Haar-like feature is the same when the non-calibrated vertical detail coefficient is applied. In other words, when a non-calibrated vertical detail coefficient is employed in the human frontal face identification method employing Haar-like features, the vertical calibration effect cannot be achieved. Therefore, prior to the calibration procedure in equation (5), the vertical detail coefficient is calibrated to zero. Equation (6) states that the zero-calibrated vertical and horizontal detail coefficients, that are multiplied by the weighting factors. Then these are calibrated from the approximation detail coefficient to produce the desired image.

$$\text{Img}_{VC}(x,y)=\begin{cases}\text{Img}_{\text{I}}(x,y), & \text{for } \text{Img}_{\text{I}}(x,y)\geq 0,\\ 0, & \text{for } \text{Img}_{\text{I}}(x,y)<0.\end{cases} \tag{4}$$

$$\text{Img}_{HR}(x,y)=\begin{cases}\text{Img}_{Hori}(x,y), & \text{for } \text{Img}_{Hori}(x,y)\geq \text{Img}_{VC}(x,y),\\ 0, & \text{for } \text{Img}_{Hori}(x,y)<\text{Img}_{VC}(x,y).\end{cases} \tag{5}$$

$$\text{Img}_{Desire}(x,y)=\text{Img}_{appx}(x,y)+2\alpha\text{Img}_{VC}(x,y)-\alpha\text{Img}_{HR}(x,y) \tag{6}$$

3.4 Face Region Detection

In this phase, key facial points such as the eyes, mouth, and nose are located. To reduce variations caused by distance between the camera and the driver, the detected face image is resized to a width of 500 pixels and converted to grayscale before being normalized for regression-tree processing (Saeed et al., 2020). The regression trees then approximate landmark positions based on pixel intensities, using gradient-boost learning to minimize squared error and applying different priors to capture facial structures. This process identifies the boundaries of the eyes, mouth, and nose, as summarized in Table 3, and the resulting facial landmarks are marked in Figure 4, with the red points used for further analysis.

Table 3. Human Facial Landmark

SL number	Parts of the Face	LandmarkPoints
1	Mouth	68–88
2	Left Eye	41–48
3	Right Eye	33–38
4	Nose	27–32

Figure 4. Landmarks on the Face

3.5 Feature Extraction

After marking the points on face, the drowsiness features are calculated in the next subsection.

3.5.1 Eye Aspect Ratio (EAR)

The primary requirement of drowsiness detection systems is to detect of eye blinking or movement. On the boundary of the eyes, there are some co-ordinates. These coordinates of eyes are utilized to calculate EAR as described in equations (7-9). Among these six coordinate positions are shown in Figure 5. ESB 32 camera is used to detect the recorded blink. After that EAR is calculated using predictive Dlib platform. In equation (10) and (11), the distance between the horizontal land mark of the eye is represented by a denominator and the vertical landmark of the eyes is represented by a numerator.

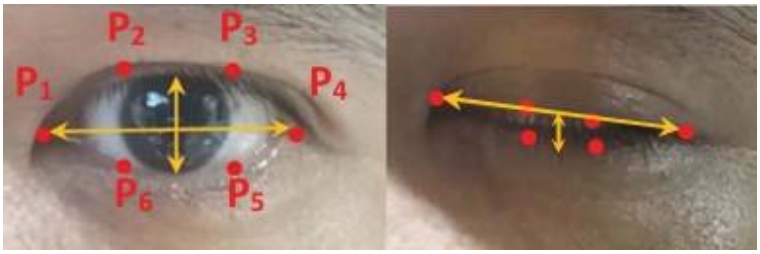

Figure 5. Labelling of Six Coordinates

As seen in Figure 5, it includes P_1, P_2, P_3, P_4, P_5, and P_6. Given that there are two sets of vertical points and only one set of horizontal points, the denominator is suitably weighted. The eye aspect ratio is approximately constant while the eye is open. In Figure 5, authors have found six different points P_1, P_2, P_3, P_4, P_5, and P_6. At first, the horizontal Euclidean distance between P_1 and P_4 is calculated using equation and the vertical Euclidean distance between P_2, P_6 and P_3, P_5 is calculated using equation (8), (9) and (10) respectively.

$$\text{Distance}(P_2, P_6) = \sqrt{(P_{2x} - P_{6x})^2 + (P_{2y} - P_{6y})^2} \quad (7)$$

$$\text{Distance}(P_3, P_5) = \sqrt{(P_{3x} - P_{5x})^2 + (P_{3y} - P_{5y})^2} \quad (8)$$

$$\text{Distance}(P_1, P_4) = \sqrt{(P_{1x} - P_{4x})^2 + (P_{1y} - P_{4y})^2} \quad (9)$$

Finally, the eye landmark distance for both eyes is calculated according to the equation (10).

$$L = \frac{\text{Distance}(P_2, P_6) + \text{Distance}(P_3, P_5)}{\text{Distance}(P_1, P_4)} \quad (10)$$

Here, *L* is the eye landmark distance. In the next step, this landmark distance from left to right eyes is calculated as per equation (11).

$$\bar{L} = \frac{l*r + l*l}{2} \quad (11)$$

Eye aspect ratio is being "Zero" dramatically when a person blinks his/her eyes. If this value remains constant for 30 frames consecutively, it indicates no movement of eyes or facial features indicating the subject is in a static pose.

3.5.2 Mouth Opening Ratio (MOR)

The Mouth Opening Ratio (MOR) is used to identify yawning behaviour, which serves as an indicator of driver drowsiness. It is calculated using the following equation (12). A high MOR value indicates that the driver's mouth is significantly open; if this elevated value persists for a certain duration, a yawning event is detected. Conversely, when the MOR value approaches zero, the driver is considered to be in a normal, non-yawning state.

$$\text{MOR} = \frac{(p_{15} - p_{23}) + (p_{16} - p_{22}) + (p_{17} - p_{21})}{3(p_{19} - p_{13})} \quad (12)$$

3.5.3 Mouth Opening Ratio (MOR)

From the existing database, authors can calculate the Eye Aspect Ratio (EAR) for three categories of eye states to determine the EAR Threshold Value. These three states are "opened", "half-closed" and "closed". However, in these datasets, only two categories-opened and closed-are included, authors have taken the most closed eyes images as "closed" and slightly opened eyes images as "half-closed". To calculate the EAR for the different eye states, here 6 points are used for each eye from 68 facial detection landmark model. When a person opens his/her eyes, that time the EAR ration is high and constant. If this value remains constant for 30 frames consecutively it indicates no movement of eyes or facial features indicating the subject is in a static pose. For each image, the corresponding points are extracted, and the EAR is calculated using equation (7).

Open States: Authors will calculate the EAR for an image from the training set. Example- the image '61072' has the following detected eye points: The detected eye points from image 61072 from dataset "Drowsiness Detection Dataset" folder; Training set are as given - P_1: (372, 200), P_2: (392, 194), P_3: (420, 198), P_4: (432, 214), P_5: (414, 221) and P_6: (389, 215).

3.5.4 Calculation of Euclidian Distances

In this subsection, Euclidian distances between P_2 and P_6, P_3 and P_5, P1 and P_4 are calculated

$$\|p_2 - p_6\| = 21.21,\ \|p_3 - p_5\| = 23.76,\ \|p_1 - p_4\| = 61.61$$

$$EAR(value\ 1) = \frac{21.21 + 23.76}{2 * 61.61} = 0.36$$

The EAR value of the Opened eye image from the dataset is 0.36. Some other EAR Values for opened eyes from the dataset are 0.34, 0.31 and 0.437.

Half-Closed States: Authors will calculate the EAR for an image from the training set. Example- an image from the datasets has the following detected eye points: P_1: (405, 119), P_2: (432, 109), P_3: (463,113), P_4: (488, 123), P_5: (459, 128) and P_6: (430, 125).

Calculation of Euclidean Distances

$|P_2 - P_6|$ = 16.12,

$|P_3 - P_5|$ = 15.52,

and

$|P_1 - P_4|$ = 83.1.

3.5.5 Calculation of Lip Distances

After extracting eye, mouth, and nose values, drowsiness is identified using SVM-based frame classification and threshold value. Thresholds for EAR, MOR, and NLR are obtained during a setup phase where the driver is assumed to be in a normal state. Around 100 - 200 frames are recorded. EAR values are used to set the eye-open threshold for same frames. If the EAR falls below this threshold, eyes are considered closed. Similarly, MOR thresholds are set from frames where the mouth is closed. Yawning is detected when the test value exceeds the threshold. NLR values (0.8 - 1 for a normal head position) are averaged to detect head bending. During testing, if any of the eye, mouth, or head indicators signal abnormal behaviour over most frames (e.g., 70 out of 75), a drowsiness alert is triggered. To simplify thresholding, a single EAR-based threshold may be used, adjusted by yawning and head-bending conditions. These threshold values are shown in table 4.

Table 4. Calculated Threshold Values for EAR, Nose and Mouth

Sl. No.	Parts of the Face	Threshold Values
1	EAR	0.30
2	Nose	Threshold=Threshold+0.002×Max bound exist
3	Mouth	Threshold=Threshold+0.001×Max bound exist

4. Result and Discussion

Step wise results are shown in this section. Table 2 describes the comparative study between the existing technique in this domain.

4.1 Related software and hardware

All software implementations are done in python. For the hardware the authors used ESP32-CAM, its a microcontroller with a camera module (OV2640). Due to the connectivity Arduino GND, ESP32-CAM GND pin (Black wire): a common ground is used. Figure 6 is showing the complete hardware connectivity.

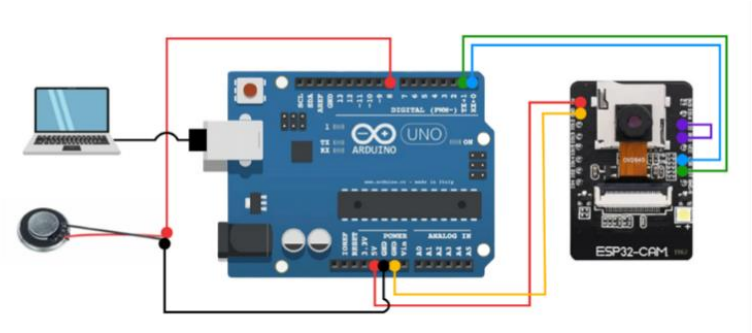

Figure 6. Hardware connectivity

4.2 Stepwise outputs

This subsection describes step-wise output after applying basic image processing operations*:*

Step 1: In the proposed method, the first step is to collect the frames (still images) from the real-time video input while driving the car. For this process the authors have used image acquisition. Figure 6 shows different types of frontal face images during driving.

Step 2: In the second step, only frontal face region is being segmented and result for the segmentation is shown in figure 7.

Step 3: In the third step, the specific region of interests (ROI) like eyes, mouth, has been segmented. The result or output for this step is shown in Figure 8.

Step 4: Next step for the process is to calculate EAR value and Yawning Detection value with the extracted the features using equation (10). Yawn value is calculated as per equation (11). To detect ywan value, authors will also use 68 (*x,y*) coordinates mapping to facial structures on the face using a method called 'shape predictor'. The corresponding image is shown in Figure 9. Most identified facial landmarks have been shown in Figure 10.

Figure 7. Image Acquisition

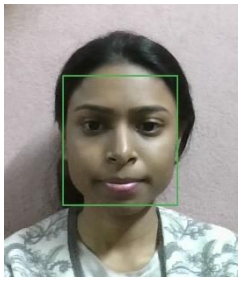

Figure 8. Face Detection

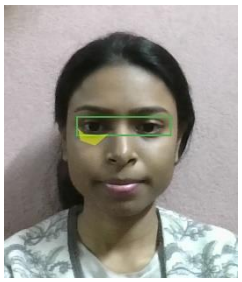

Figure 9. Image Segmentation

Figure 10. Facial Landmark Detection

Results: Depending on some parameters like extracted features, eyes movement, mount movements the system determines if the driver is in drowsy state or not. If drowsiness is detected, it gives an alert. Calculated Threshold Values are YAWN-THRESH = 20 and EYE-AR-THRESH = 0.3. Figure 11 shows the Ear and Yawn threshold value against the given input image.

No Alarm: This image is showing the values for EAR and Yawn with no Drowsiness alert as these values didn't cross the threshold values.

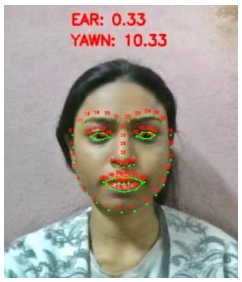

Figure 11. Image Analysis

Alarm: Here, in the attached images, for the first image, a Yawning Alert is given as the Yawn value (29)> Threshold Value (20). In the second image, Drowsiness Alert is given as EAR value (0.19) < Threshold value (0.3). Figure 12 shows yawn alert along with drowsiness alert.

Figure 12. Yawn alert and Drowsiness alert

So, the method is working accurately. Authors have also tested the proposed technique by taking different sets of data. Table 5 is showing the result based on the drowsiness detection accuracy.

Table 5. Performance accuracy on different data sets

Method Name	Number of tests taken	Number of Positive detections	Number of negative detections	Detection accuracy
Proposed Method	35	34	1	97.14%
	43	40	3	93.12%
	57	55	2	96.49%
	50	50	0	100%
Total Data Sets	185	179	6	Average Detection Accuracy - 96.75%

Table 6 describes the comparative studies between exiting methods and the proposed methods with respect to RMSE, Dice index measure, precision and accuracy metrics. The metric like RMSE, Dice Index Measure, Precision and Accuracy (Datta et al., 2019) are evaluated. A detailed description of these metrics can be found in Saeed et al. (2020) and Datta et al. (2023).

Table 6. Performance analysis with other existing methods based on popular metric

Sl number	Method Name	Used Methodology	Root Mean Square Error (RMSE)	Dice Index Measure	Precision (%)	Accuracy (%)
1	Luo et al. (2013)	LBP and SVM	1.12	0.89	91.45	90.23
2	Kawashima (2021)	Appearance Model (AAM) and 3D coordinate features	0.89	0.83	87.92	89.77
3	Arunpandian and Gunasekaran (2024)	MTCNN+MC-KCF	0.78	0.90	90.67	92.89
4	Proposed Method	Modified Haar Cascade and Feature extraction	0.98	0.91	93.5	96.78

Figure 13 shows the comparison between RMSE and Dice Index Coefficient and Figure 14 graphically presented the comparison with respect to Precision and Accuracy.

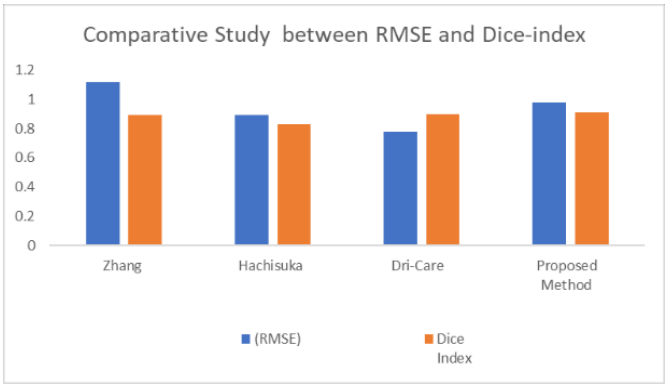

Figure 13. Comparison between RMSE and Dice Index

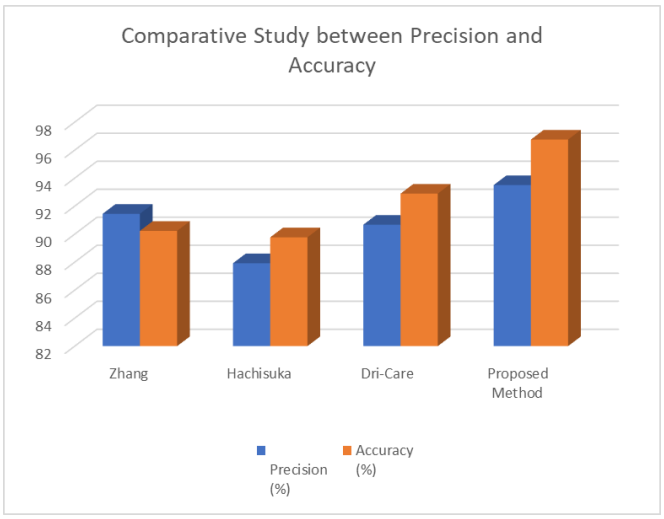

Figure 14. Comparison w. r. t. Precision and Accuracy

5. Conclusions

A new automatic technique is presented throughout the study to identify whether the drivers of the automobiles are sleepy or not. The authors demonstrated how the mean distance between eye landmarks can be calculated from the position of facial landmarks, which is helpful in figuring out the blinking pattern of the eyes. It could be readily distinguished between drowsy and non-drowsy drivers based on the eye blinking pattern. The personal computer processes the entire driver drowsiness detection system. This device detects drowsiness in real time. After testing our algorithm on the aforementioned 29 drivers, authors were able to attain nearly 94.5% accuracy rate. An alarm mechanism was created to alert the driver when the sleepy driver was classified. However, the proposed technique should not able to detect drowsiness of the driver when he/she wears sunglasses, hats, masks, or hair can block key facial landmarks (eyes, mouth). This proposed technique would not work in the presence of low light. In the future, authors will be working on these limitations along with expected to expand the system to identify not only tiredness but also other behaviours that may contribute to a collision, such talking on a cell phone or sitting next to a driver.

Acknowledgements

Authors are thankful to Sister Nivedita University for providing infrastructural support.

References

ANSI/ASHRAE Standard 55 (2023). Thermal Environmental Conditions for Human Occupancy. https://www.ashrae.org/technical-resources/bookstore/standard-55-thermal-environmental-conditions-for-human-occupancy, Accessed 14 August 2025.

Arunpandian, J., & Gunasekaran, V. (2024). Enhanced Road Safety Through Intelligent Lane Detection and Driver Drowsiness Monitoring. 2024 15th International Conference on Computing Communication and Networking Technologies (ICCCNT) (pp. 1-7). Kamand: IEEE.

Bakheet, S., & Al-Hamadi, A. (2021). A Framework for Instantaneous Driver Drowsiness Detection Based on Improved HOG Features and Naïve Bayesian Classification. Brain Sciences, 11(2), 240.

Biswas, S., Saha, T., Banerjee, P., & Datta, S. (2023). A novel facial emotion recognition technique using convolution neural network. In Singh, P., Singhal, P., Mishra, P. K., & Vatsa, A. K., Heterogeneous Computational Intelligence in Internet of Things (pp. 175–195). Boca Raton: CRC Press.

Chen, S., Wang, Z., & Chen, W. (2021). Driver Drowsiness Estimation Based on Factorized Bilinear Feature Fusion and a Long-Short-Term Recurrent Convolutional Network. Information, 12(1), 3.

Choudhury, P., Thakur, K., & Datta, S. (2023). An application of convolutional neural networks in recognition of handwritten digits. In Singh, P., Singhal, P., Mishra, P. K., & Vatsa, A. K., Heterogeneous Computational Intelligence in Internet of Things (pp. 261–276). Boca Raton: CRC Press.

Datta, S., & Chaki, N. (2015). Detection of dental caries lesion at early stage based on image analysis technique. 2015 IEEE International Conference on Computer Graphics, Vision and Information Security (CGVIS) (pp. 89-93). Bhubaneswar: IEEE.

Datta, S., Chaki, N., & Modak, B. (2019). A Novel Technique to Detect Caries Lesion Using Isophote Concepts. IRBM, 40(3), 174–182.

Datta, S., Chaki, N., & Modak, B. (2023). A novel technique for dental radiographic image segmentation based on neutrosophic logic. Decision Analytics Journal, 7, 100223.

Dua, H. K., Goel, S., & Sharma, V. (2018). Drowsiness detection and alert system. 2018 International Conference on Advances in Computing, Communication Control and Networking (ICACCCN) (pp. 621-624). Greater Noida: IEEE.

Ed-Doughmi, Y., Idrissi, N., Hbali, Y. (2020). Real-Time System for Driver Fatigue Detection Based on a Recurrent Neuronal Network. Journal of Imaging, 6(3), 8.

Fahmy, H. (2023). Drowsiness detection dataset: UnityEyes - Openned/Closed Eyes - Sleepy Driver Detection. https://www.kaggle.com/datasets/hazemfahmy/openned-closed-eyes, Accessed 3 November 2025.

Global status report on road safety 2018. (2018). Geneva: World Health Organization. file:///C:/Users/p-c/Downloads/9789241565684-eng.pdf, Accessed 18 August 2025.

Horne, J., & Reyner, L. (1999). Vehicle accidents related to sleep: A review. Occupational and Environmental Medicine, 56(5), 289–294.

Jebraeily, Y. (2023). Drowsy Detection Dataset: Stay Awake, Stay Safe: A Dataset for Drowsiness Detection on Kaggle. https://www.kaggle.com/dsv/8311245, Accessed 17 August 2025.

Kawashima, H. (2021). Active appearance models. In Ikeuchi, K. (Ed.), Computer Vision: A Reference Guide (pp. 11-15). Cham: Springer.

Kolus, A. (2024). A Systematic Review on Driver Drowsiness Detection Using Eye Activity Measures. IEEE Access, 12, 97969-97993.

Kolus, A., Wells, R. P., & Neumann, W. P. (2023). Examining the relationship between human factors related quality risk factors and work related musculoskeletal disorder risk factors in manufacturing. Ergonomics, 66(7), 954-975.

Lenin, N. C., Padmanaban, S., Bhaskar, M. S., Mitolo, M., & Hossain, E. (2021). Ceiling Fan Drives–Past, Present and Future. IEEE Access, 9, 44888-44904.

Luo, Y, WU, C-m, & Zhang, Y. (2013). Facial expression feature extraction using hybrid PCA and LBP. The Journal of China Universities of Posts and Telecommunications, 20(2), 120-124.

Magán, E., Sesmero, M. P., Alonso-Weber, J. M., & Sanchis, A. (2022). Driver Drowsiness Detection by Applying Deep Learning Techniques to Sequences of Images. Applied Sciences, 12(3), 1145.

Mohana, B., & Sheela Rani, C. M. (2019). Drowsiness Detection Based on Eye Closure and Yawning Detection. International Journal of Recent Technology and Engineering, 8(4), 8941–8944.

Moujahid, A., Dornaika, F., Arganda-Carreras, I., & Reta, J. (2021). Efficient and compact face descriptor for driver drowsiness detection. Expert Systems with Applications, 168, 114334.

Patil, P. V. (2020). Drowsiness detection dataset: Classify based on whether eyes are closed or open. https://www.kaggle.com/datasets/prasadvpatil/mrl-dataset, Accessed 29 December 2024.

Rastogi, A., & Ryuh, B. S. (2019). Teat detection algorithm: Yolo vs. Haar-cascade. Journal of Mechanical Science and Technology, 33(4)1869–1874.

Saeed, K., Datta, S., & Chaki, N. (2020). A Granular Level Feature Extraction Approach to Construct HR Image for Forensic Biometrics Using Small Training DataSet. IEEE Access, 8, 123556-123570.

Singh, J., Kanojia, R., Singh, R., Bansal, R., & Bansal, S. (2023). Driver drowsiness detection system: An approach by machine learning application. arXiv preprint: https://doi.org/10.48550/arXiv.2303.06310.

Zhang, W., Cheng, B., & Lin, Y. (2012). Driver drowsiness recognition based on computer vision technology. Tsinghua Science and Technology, 17(3), 354-362.